



11th Canadian Masonry Symposium, Toronto, Ontario, May 31- June 3, 2009

CONFINED MASONRY – A CHANCE TO IMPROVE THE LOAD BEARING CAPACITY

W. Jäger¹ and P. Schöps²

¹ Professor, Chair of Structural Design, Faculty of Architecture, Technische Universität Dresden,
Lehrstuhl.Tragwerksplanung@mailbox.tu-dresden.de

² Research Assistant, Faculty of Architecture, Technische Universität Dresden,
Peter.Schoeps@mailbox.tu-dresden.de

ABSTRACT

With the introduction of the semiprobabilistic safety concept with partial factors for masonry design in Germany an increase of the horizontal action due to wind- and seismic loads is connected (s. 1). This fact was overlaid by the reduction of the number and area of stiffening walls from the point of view of economy as well as by lowering the bulk density to achieve a higher thermal insulation. The latter leads to a reduction of the available strength of the units also. Therefore considerable research efforts have been made in Germany to compensate the losses of bearing capacity and to guarantee the competitiveness of masonry with other building materials (s. 2 - 6). Confined masonry is an adequate alternative – besides the execution as reinforced masonry – in order to increase the design resistance. It has until now found only a low application in Germany. That's why it was taken into account in the efforts to increase the load bearing capacity of stiffening walls by the research project presented in the following.

Due to the encapsulation of a masonry wall with a reinforced concrete frame the behaviour under horizontal actions improves considerably in case of confined masonry. As part of a research project cyclic tests performed on walls made of autoclave aerated concrete units encased by a reinforced concrete framework will be presented below. Parallel to the large scale wall tests a detailed determination of the material parameters for the purpose of a numerical modelling was done. The simulation shows in detail the forces in the wall and the interaction between masonry and the reinforced concrete frame. Finally a proposal for the efficient design is presented. A comparison with conventional masonry shows especially for small loads a significant gain of shear load capacity. Even the ductility, which is particularly important for earthquake design, is significantly higher than for common stiffening walls. But the difference in erection compared to infill masonry is low. The confined masonry leads to a much better connection between masonry and concrete frame and thus the extra vertical loads, which are very important for masonry, can be activated. The association of masonry and concrete leads to stable and affordable buildings.

In the following interesting test results with confined masonry will be presented and discussed. They show some reserves in the interpretation and application of load-bearing reserves could be use in the future.

KEYWORDS: confined masonry, cyclic shear tests, effect of shrinkage, numerical simulation

INTRODUCTION

Confined masonry was in the past and is in the present a continuous matter of research interest to understand the structural behaviour as well as to simplify the design methods for the practices without any complicated numerical tools (s. 3). In the following some new aspects were introduced in the research focus like the shrinkage of the RC-frame and the location of the zero point of moment.

Confined masonry differs both from reinforced masonry and from infill masonry. The most essential difference in comparison with infill masonry consists in the fact that the masonry carries a portion of the vertical load. The sequence in the erection of the structural members is therefore an important factor for confined masonry. In skeleton structures with infill masonry the RC-frame is fabricated first and afterwards comes the infill. For confined masonry the order is reversed. This has a direct effect on the bond strength between frame and masonry as well as on the vertical load upheld by the masonry.

Masonry units with vertical holes or openings are used in the case of reinforced masonry with vertical rebars. The openings or holes foreseen for the rebars are filled with concrete during or after erection of the masonry wall. At the end of the construction process the masonry is confined by reinforced concrete. This confinement however does not possess shear reinforcement and is not a real frame able to carry horizontal loads without the masonry infill. However, the increased load bearing capacity for bending due to inplane loads of the whole wall is also an effect of confinement.

Confined masonry combines the positive properties of both construction types and can achieve higher load-carrying capacities under static as well as under seismic actions.

For the numerical simulation the ANSYS-Software was used with a special developed interface model to describe the behaviour close to the reality.

EXPERIMENTAL TESTS

For the assessment of the shear load capacity of confined masonry four test were carried out with masonry made of autoclaved aerated concrete (AAC). In this connection the special behaviour of this construction type was examined as compared to common stiffening walls. The aim was to assess the shear load behaviour of a masonry wall confined by reinforced concrete along with the pre-stressing effects caused by different processes of shrinkage.

The reinforcement of the RC-frame followed the least requirements of the German earthquake code DIN 4149. The thickness of the frame corresponded to the thickness of the masonry of 24 cm. For the masonry were used units of the strength category 4 ($f_{bk} = 4 \text{ N/mm}^2$), dimensions $50 \text{ cm} \times 24 \text{ cm} \times 25 \text{ cm}$ and overlapping length of a half unit. The bed joints were made with thin layer mortar and the head joints were unfilled.

The deformation of the test specimens were measured after the erection and prior to the testing, as well as during the test process. In the period after the production the deformations due to shrinkage were measured with mechanical extensometers on the surface of the test walls and with digital meters at the end of steel bars, which were placed in cladding tubes inside of the RC-frame. The arrangement of the measuring points is shown in Figure 2:.

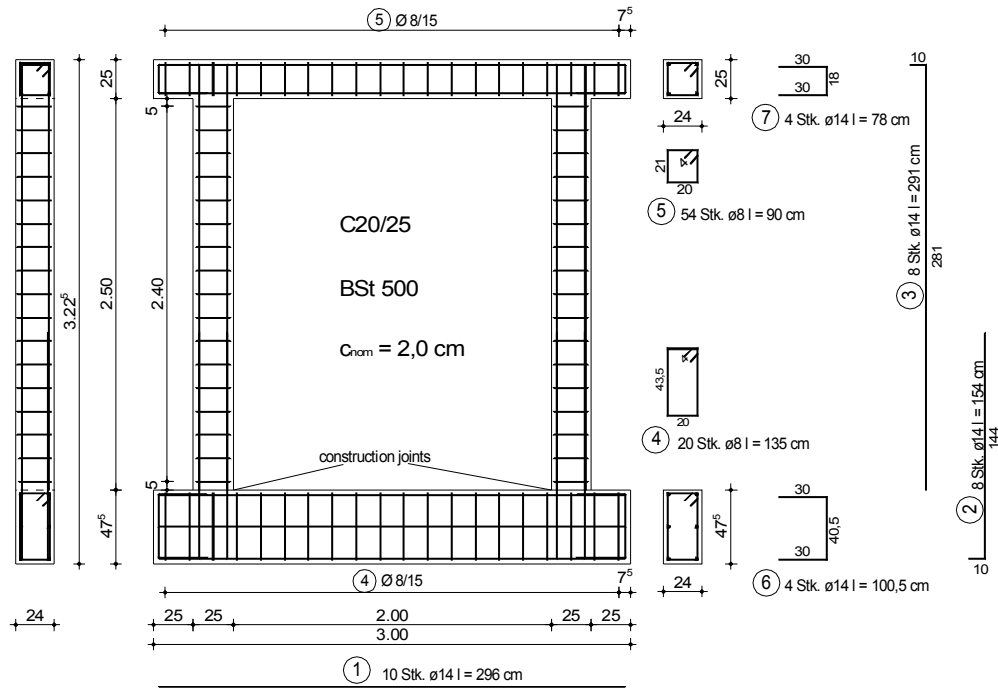


Figure 1: Reinforcement drawing (length in cm; diameter in mm)

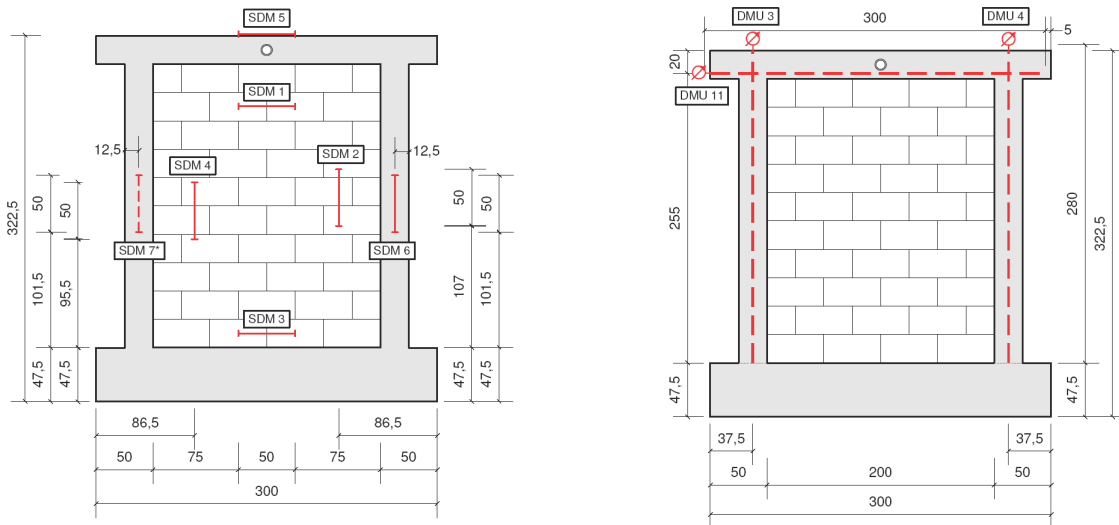


Figure 2: Plan of measurement points for shrinkage of the wall (left: mechanical extensometer; right: steel bars in cladding tubes with digital meter)

The concrete of the upper beams was cast several days after the columns. The measurement of the length changes could only start on day 21 after the casting of the columns because of the formwork. An essential part of the shrinkage had already happened at that time. The length changes in the columns were therefore smaller than in the upper beam. This is also to be recognised by the lower increase rate of the curves at the beginning. For the walls 1 and 2 approximately -0.2 mm and for the walls 3 and 4 approximately -0.3 mm are to be added for a proper comparison. The shortening observed at all places results from the shrinkage of the

concrete respectively from the resulting compression strain in the masonry part. The precompression of the masonry could be reproduced numerically (see below).

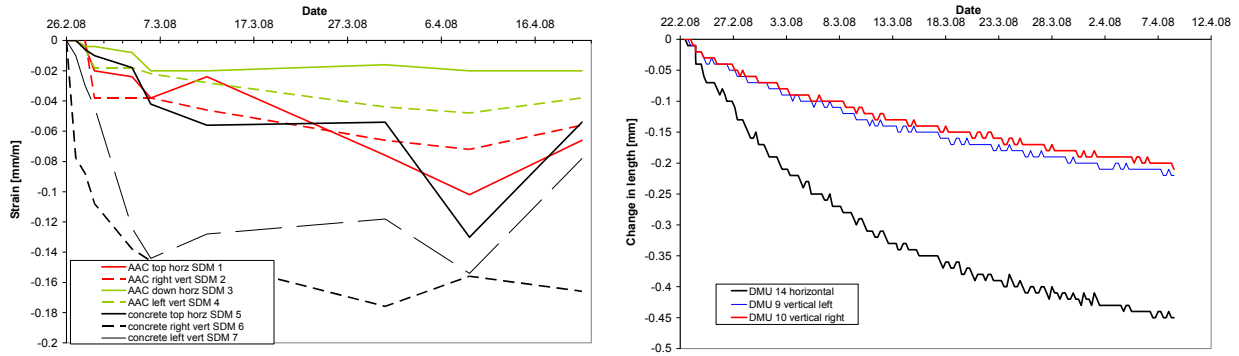


Figure 3: Deformation due to shrinkage for wall 4 (left: mechanical extensometer; right: steel bars in cladding tubes with digital meter)

With the test arrangement for the shear tests two variants were examined. With the first variant only a constant vertical load was applied on the test walls. Therefore the external point of zero moment lies at the top of the wall. For the last test both vertical cylinders were computer controlled to keep the external point of zero moment at the half wall height. So the load of both cylinders is partially different, but the total load has a constant value. In the shear test the vertical load were applied during the first load step. In the second step a cyclic horizontal displacement was imposed at the top. This was increased after every third cycle. Figure 4: shows the typical first cracks.

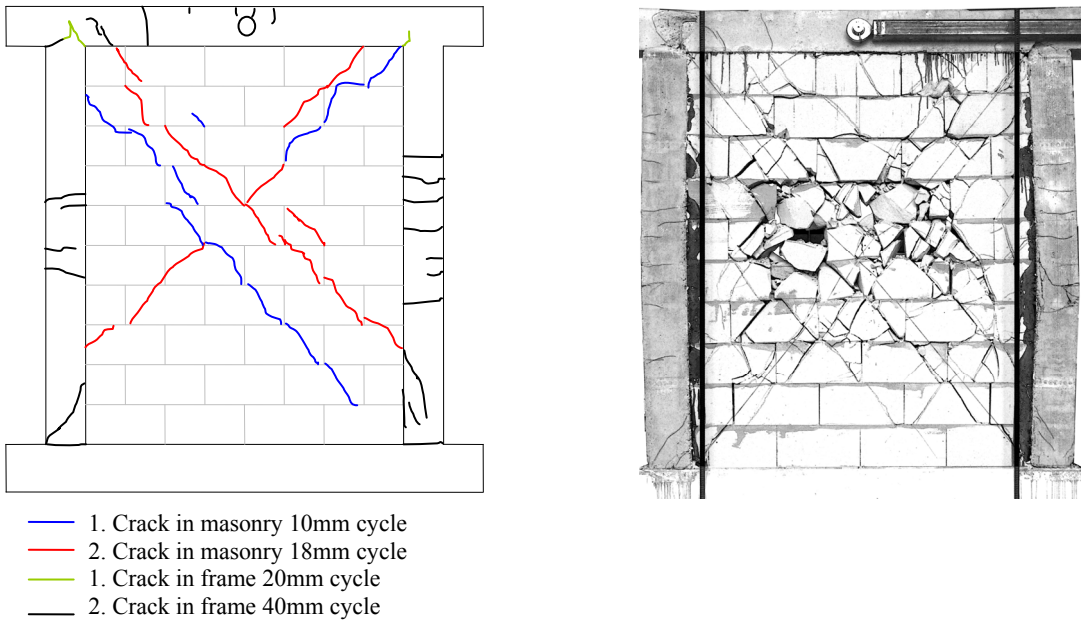


Figure 4: Typical crack pattern (wall 2)

On the right side of Figure 4: is shown the crack pattern at the end of the test. The shear resistance in the last cycle is still higher than that of a frame without masonry. Partially the displacement capacity of the test equipment was reached. A further increasing of the horizontal displacement was possible in all tests.

For the evaluation of the ductility the envelope of the hysteresis of the load-displacement-diagram has to be simplified to a bilinear curve. This is shown for all four hysteresis in the following picture. The shown displacements are the relative ones between the upper and the lower beams. These were measured with a separate decoupled measuring frame.

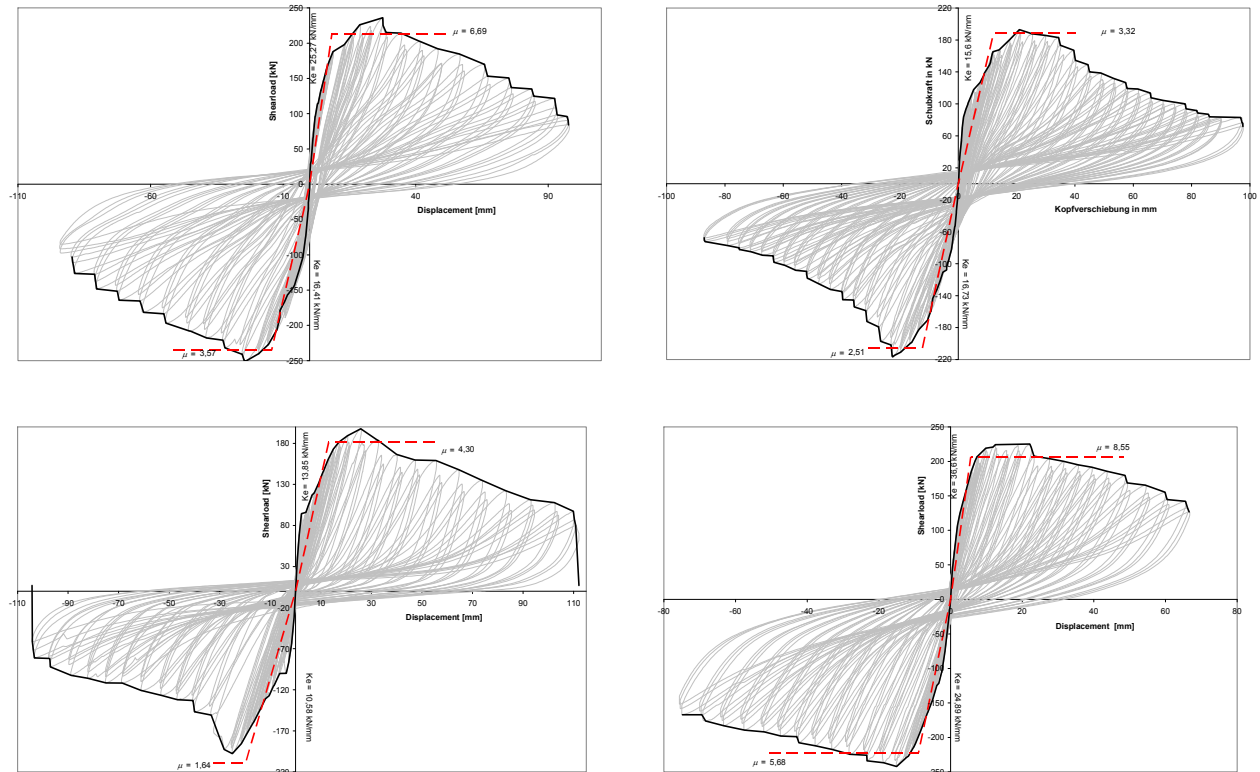


Figure 5: Force-displacement -hysteresis - envelopes und the bilinear simplification (top left: wall 1, right: wall 2, down left: wall 3, right: wall 4, dashed line: bilinear curve)

The initial stiffness is in the common approach determined at 70% of the maximum shear load. For the maximum usable displacement the point of 80% of the maximum shear load on the declined part of the envelope has to be used. The maximum load of the bilinear simplification is given by the equality of the enclosed area of both curves. In Table 1 are listed the essential results of the test.

By the distinctive non-linear characteristics of the load-deformation-curves in the rising part a larger plastic displacement is reached at 70% of the maximum shear load. This leads formally to a lower initial stiffness and much lower ductility. The values of d_{cr} are between 4.3 mm and 13.1 mm and would already equal the maximum displacement for the case of normal masonry.

Hence the observed first crack load is used in Table 2 for the calculation of the ductility and not 70% of the maximum load. So the value for the ductility becomes much higher.

An essential potential of confined masonry remains unused by the restriction of the usable area to the load-carrying capacity of 80%, because an increasing of the displacement at the top of the wall is possible and the load still lies clearly above that of conventional walls.

Table 1: Overview of the shear test results

Wall	vert. Load	H_{\max}^-	H_{\max}^+	$d_{H_{\max}^-}$	$d_{H_{\max}^+}$	70% H_{\max}^-	70% H_{\max}^+	d_{cr}^-	d_{cr}^+	K_e^-	K_e^+
	kN	kN	kN	mm	mm	kN	kN	Mm	mm	kN/mm	kN/mm
1	330	250	236	24.3	24.5	175	165	10.7	6.5	16.4	25.3
2	132	217	193	22.5	20.9	152	135	9.1	8.7	16.7	15.6
3	-	198	198	25.1	26.0	138	138	13.1	10.0	10.6	13.9
4	330	242	225	15.0	22.1	170	158	6.8	4.3	24.9	36.6

Wall	80% H_{\max}^-	80% H_{\max}^+	d_u^-	d_u^+	H_u^-	H_u^+	d_e^-	d_e^+	μ^-	μ^+
	kN	kN	mm	mm	kN	kN	mm	mm		
1	200	189	51.4	52.0	235	213	14.3	8.4	3.58	6.18
2	173	154	30.8	40.2	206	189	12.3	12.1	2.51	3.32
3	158	158	32.5	56.3	210	181	19.8	13.1	1.64	4.30
4	194	180	50.6	48.3	222	207	8.9	5.6	5.68	8.55

Table 2: Ductility with observed first crack load

Wall	H_{cr}^-	H_{cr}^+	d_{cr}^-	d_{cr}^+	K_e^-	K_e^+	H_u^-	H_u^+	d_e^-	d_e^+	μ^-	μ^+
	kN	kN	mm	mm	kN/mm	kN/mm	kN	kN	mm	mm		
1	100	97	2.4	2.2	41.3	44.9	213	204	5.2	4.6	9.95	11.42
2	107	116	4	5.1	26.7	22.8	185	177	6.9	7.8	4.43	5.18
3	86	87	2.7	2.1	31.9	41.8	158	166	4.9	4	6.56	14.18
4	125	124	3.8	2.6	32.5	47.6	217	204	6.7	4.3	7.59	11.28

In Figure 6: the observed loads are compared with actual results for conventional AAC-walls. The wall dimensions are identical for all tests resp. were projected on a uniform wall thickness. The conventional walls, which were used for the comparison, were fully fixed at the top of the wall. With the attempt of a cantilever-system the load-bearing capacity would clearly decrease in contrast to confined masonry.

In all four tests no joint failure could be observed. Also the bond between masonry and RC-frame remained intact through the whole test procedure. The failure always happened in the stone units. So the tensile strength of the unit gives the limit for the shear load capacity.

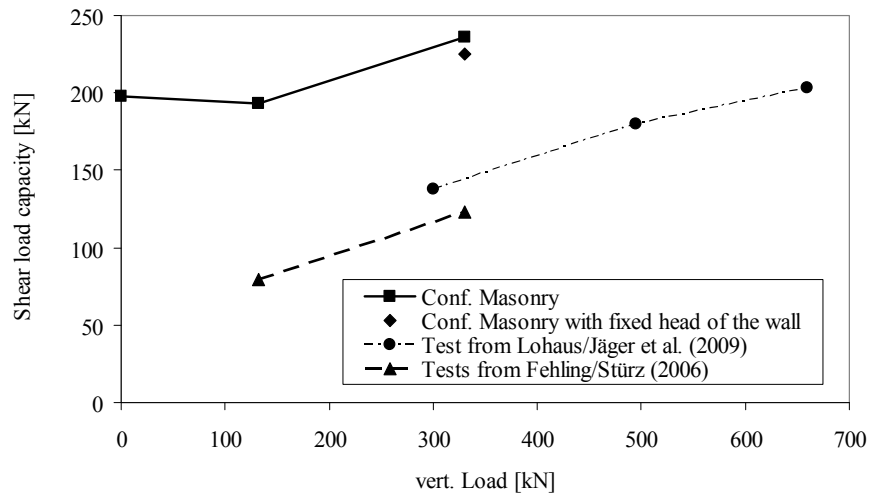


Figure 6: Comparison of ultimate shear load with results for unreinforced AAC shear walls

NUMERICAL INVESTIGATIONS

The appropriate parameters for the numerical calculation of the test were determined in small “material”-tests parallel to the wall tests. In order to obtain the values of the material point some of the small tests have also been recalculated with a numerical model. The relevant material characteristics, which were used for the numerical simulation of the cyclic shear test, are summarised in Table 3.

Table 3: Input values for numerical analyses

	Parameter		Value
Masonry Unit	Density	γ_{wb}	5.5 kN/m ³
	Compressive Strength	f_b	4.58 N/mm ²
	Tensile Strength	f_{bt}	0.88 N/mm ²
	Poisson's ratio	ν_b	0.14
	Young's Modulus	E_b	1655 N/mm ²
	Fracture Energy	G_{Ib}	10 N/m
Mortar	Tensile Strength	f_{mt}	2.59 N/mm ²
	Young's Modulus	E_m	6808 N/mm ²
	Poisson's ratio	ν_m	0.17
Bond	Shear strength	f_{vko}	1.1 N/mm ²
	Tensile Bond Strength	f_t	0.84 N/mm ²
	Friction Coefficient	μ	0,84 N/mm ²
Concrete	Density	γ_{wc}	22.8 kN/m ³
	Young's Modulus	E_c	27185 N/mm ²
	Compressive Strength	f_c	36.7 N/mm ²
	Tensile Strength	f_{ct}	2.51 N/mm ²
	Poisson's ratio	ν_c	0.2
	Fracture Energy	G_{Ic}	275 N/m
	Reinf.	Yield Stress	f_y
Tensile Strength		f_{stt}	640 N/mm ²
Young's Modulus		E_{st}	200000 N/mm ²

The program system ANSYS[®] 7 used for the numerical investigations allows to integrate user developed elements or material routines by means of a program interface. Because the typical behaviour of masonry under shear is essentially characterized by joint failure and a softening unit

failure, different interface elements were implemented within the scope of the research project. In addition a material routine was developed for the available two-dimensional elements; this however shall not be further discussed in this paper.

The deformations due to shrinkage as well as the external vertical loads were applied within the first numerical load step. A preliminary investigation proved that up to the time of the test procedure approximately 20-25% of the final shrinkage of an unloaded concrete were to be registered. In this connection plastic strains of the fresh concrete are included.

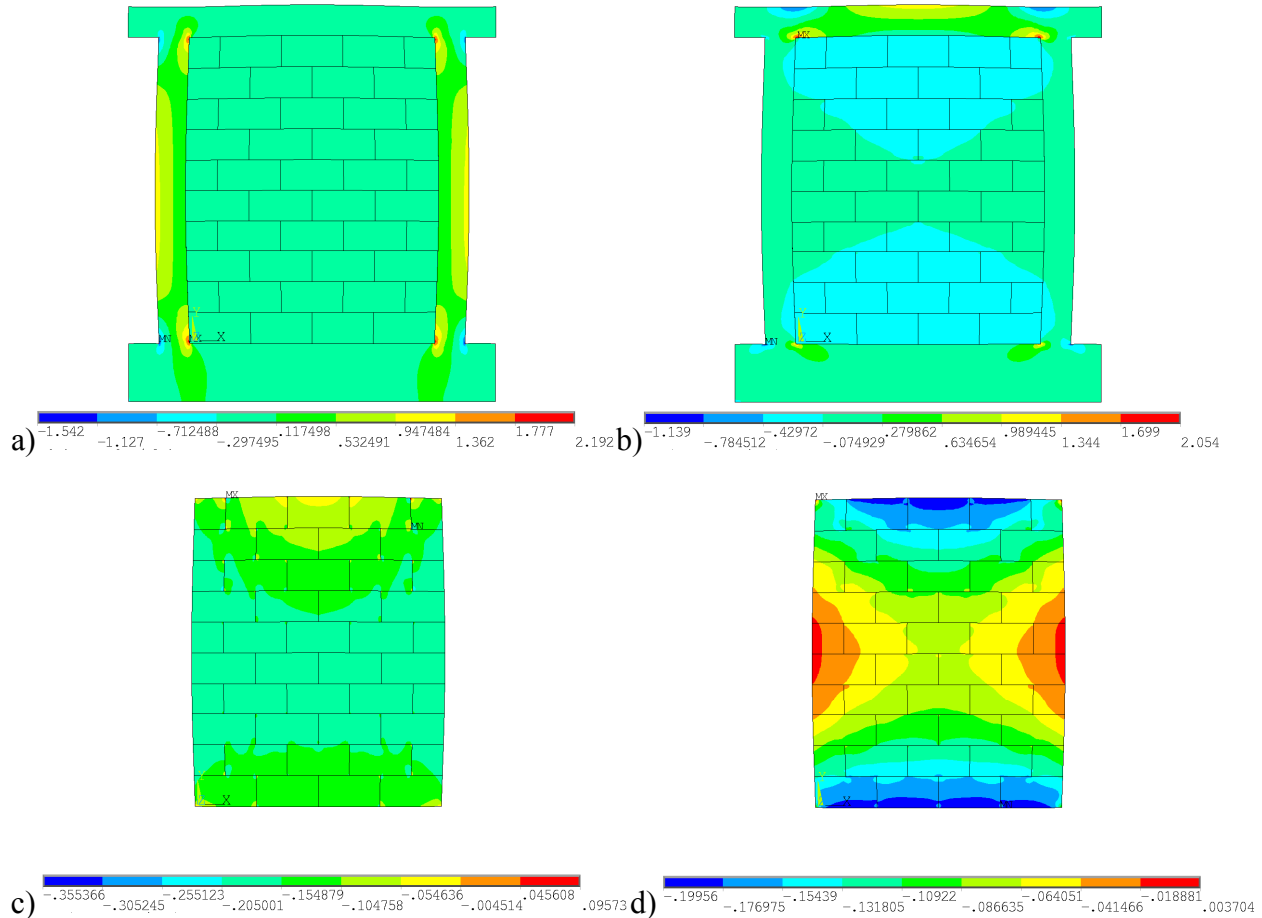


Figure 7: Stress state due to 20% shrinkage (a), c): vertical stress; b), d): horizontal stress)

The resulting stresses in the masonry remained clearly below its strengths. But in the concrete it almost reached the tensile strength. As expected, the intensity of the shrinkage influences the prestressing of the masonry and with it the shear load capacity. The horizontal shrinkage of the upper beam also induces extra shear stresses in the masonry. This leads to a reduction of the load-carrying capacity. The additional vertical load as a result of the shrinkage amounted for the masonry approximately 86 kN.

The following picture shows a typical numerical crack pattern. Compared with unconfined

masonry the cracks are fanned out clearly wide and also the stress distribution in the masonry is more homogeneous. In Figure 4: is to be seen that the first cracks goes diagonally through the masonry and both resulting wall halves are held together by the frame. With the most unfavourable estimation that both wall halves take the same portion of the shear load a shear action arises for the frame by the half height of the external shear load.

The joint failure could be examined only numerically, because the bond strength of the used AAC-unit is greater than the tensile strength of the units. The failure type varies depending on the unit geometry, the vertical load and the relation of tensile bond strength to the initial shear strength. The gapping shown on the right in Figure 8: must not lead to failure in the case of confined masonry, but rather to an additional load of the frame.

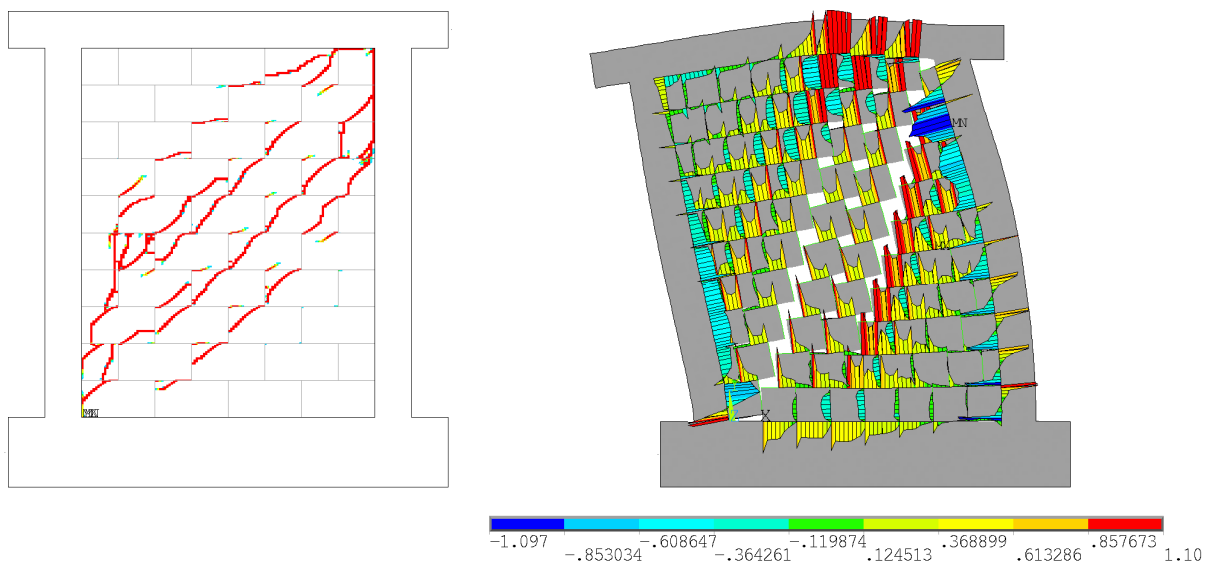


**Figure 8: Left: numerical crack pattern for a tested wall (monotonic static loading)
Right: Joint failure for shorter masonry unit without unit failure (normal stress, compression is positive)**

CONCLUSIONS

The performed wall tests clearly show the increasing effect of confinement on the load-bearing capacity to a stiffening wall made of masonry units. In this connection it could be shown that on the one hand a very good bond is achieved by casting the concrete after the erection of the masonry part, and on the other hand that a considerable precompression on the masonry is induced by the shrinkage of the concrete-frame. With higher vertical loads the cracks due to shrinkage in the frame become smaller or are closed and the amount of the vertical load upheld by the masonry becomes higher. Besides the higher vertical load the roughly constant distributed shear stress in the masonry infill also leads to a higher shear load-bearing capacity, which lies over the capacity of conventional masonry walls.

Another important advantage of confined masonry is its high ductility, which manifests itself primarily in the maximum reachable displacements with a still high shear resistance. The ductility μ calculated in the common approach does not reflect this quality adequately. Here the

area below the envelope of the load-displacement-relation delivers, if necessary, a better comparability for the different construction types.

The design can be based on the design equations for unreinforced masonry. The constant shear stress distribution can be taken into account by means of a factor or a higher compressive length. Additionally verifications of the frame have to be performed as well.

Because the external static system has no decisive influence on the shear load-bearing capacity of the confined masonry, the calculation can be simplified and is comparable with this one for pure masonry buildings. No exact calculation of the internal forces with regard to the moment distribution in the stiffening wall is necessary. A complex building modelling can be avoided. Merely the anchoring to downward has to be checked.

The tests carried out on shear wall specimens within the scope of this project are limited to AAC masonry. Additional tests with other types of units are necessary for a generalization. In this cases the bond behaviour can be another one as well as the tensile failure of the units.

ACKNOWLEDGEMENTS

This research project was carried out with the financial support of the Federal Office for Building and Regional Planning Germany and the Federal Association of AAC Germany. The tests were done with the friendly support of Xella Technology- and Research Centre Emstal.

REFERENCES

1. DIN 4149: *Bauten in deutschen Erdbebengebieten: Lastannahmen, Bemessung und Ausführung üblicher Hochbauten*. DIN Beuth Verlag: Berlin April 2005.
2. Meyer, U. et al: Different Contributions to the ESECMaSE Project (esp. Sessions 1C and 2C). In: *Proceedings of the 14th International Brick & Block Masonry Conference*, 14-17 February 2008, Sydney, Australia.
3. Al-Chaar, G.; Mehrabi, A.B.; et al.: Finite Element Interface Modelling and Experimental Verification of Masonry-Infilled R/C Frames. *TMS Journal* 26 (2008) 1, pp. 47 - 65.
4. Jäger, W.; Schöps, P. (2009): *Eingefasstes Mauerwerk als Möglichkeit zur Erhöhung der Tragfähigkeit von Aussteifungswänden*. Research Report. Technische Universität Dresden, Chair of Structural Design, Faculty of Architecture.
5. Fehling, E.; Stürz, J. (2006): *Experimentelle Untersuchungen zum Schubtragverhalten von Porenbetonwandscheiben*. Research Report. Universität Kassel, Institut für Konstruktiven Ingenieurbau, Fachgebiet Massivbau.
6. Lohaus, L.; Jäger, W.; Höveling, H.; Steinborn, T.; Schöps, P. (2009): *Schubtragfähigkeit von Mauerwerk aus Porenbeton-Plansteinen und Porenbeton-Planelementen*. Forschungsbericht. Hannover u. Dresden.
7. ANSYS® Academic Research, Release 11.0, ANSYS, Inc.